DESIGN AND CHARACTERIZATION OF A PASSIVE WIRELESS DNA SENSOR

Haibo Xu, Yi Jia, Lisandro Cunci
Department of Mechanical Engineering
University of Puerto Rico - Mayaguez

What is DNA molecule?

What does “passive” and “wireless” mean?

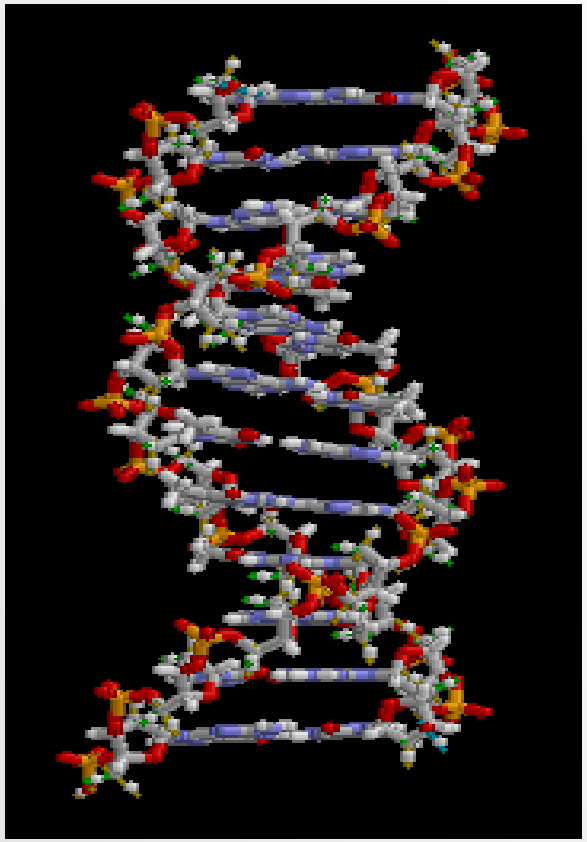

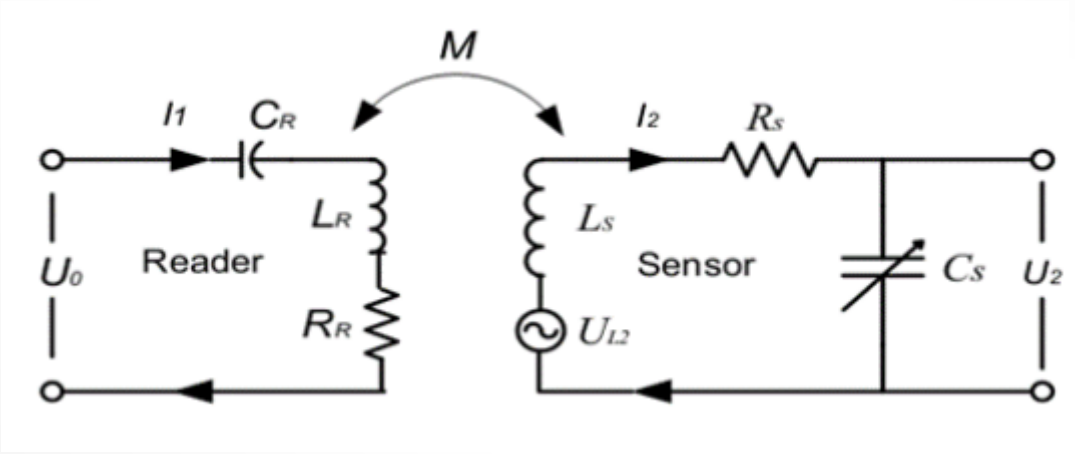

INTRODUCTION

Advancements in DNA research has lead scientist discover practical new uses for this molecule ranging from genetic expression detection to metal ion detection. Being able to synthesize any DNA sequence has made the molecule useful to identify specific genetic mutations by means of hybridization; consequently label free hybridization detection is of great interest due to its simple implementation with CMOS technology. Similar types of biosensors for biological agents quantification has been demonstrated such as bacterial as well as impedance studies on ssDNA (single strand DNA) immobilized on bare gold. Furthermore, reliable DNA immobilization techniques are necessary for further commercialization of label free ssDNA hybridization detection technology.

Devices like planar interdigitated array of microelectrodes (IDAM) present a solution to this problem, providing a flat surface for simple chemical manipulation and easy electrical readout implementation. The primary goal of the proposed research is to conduct basic research into DNA capacitive sensing mechanism and DNA/surface interfacial conformational characterization during DNA hybridization process with passive wireless integrated RFID sensor technologies in order to develop an innovative DNA sensing platform for environmental and biomedical applications. Before we prepare for discussing the principle of interdigital capacitive sensors (IDC-S), approximation model should be briefly illustrated in Fig 1 as below.

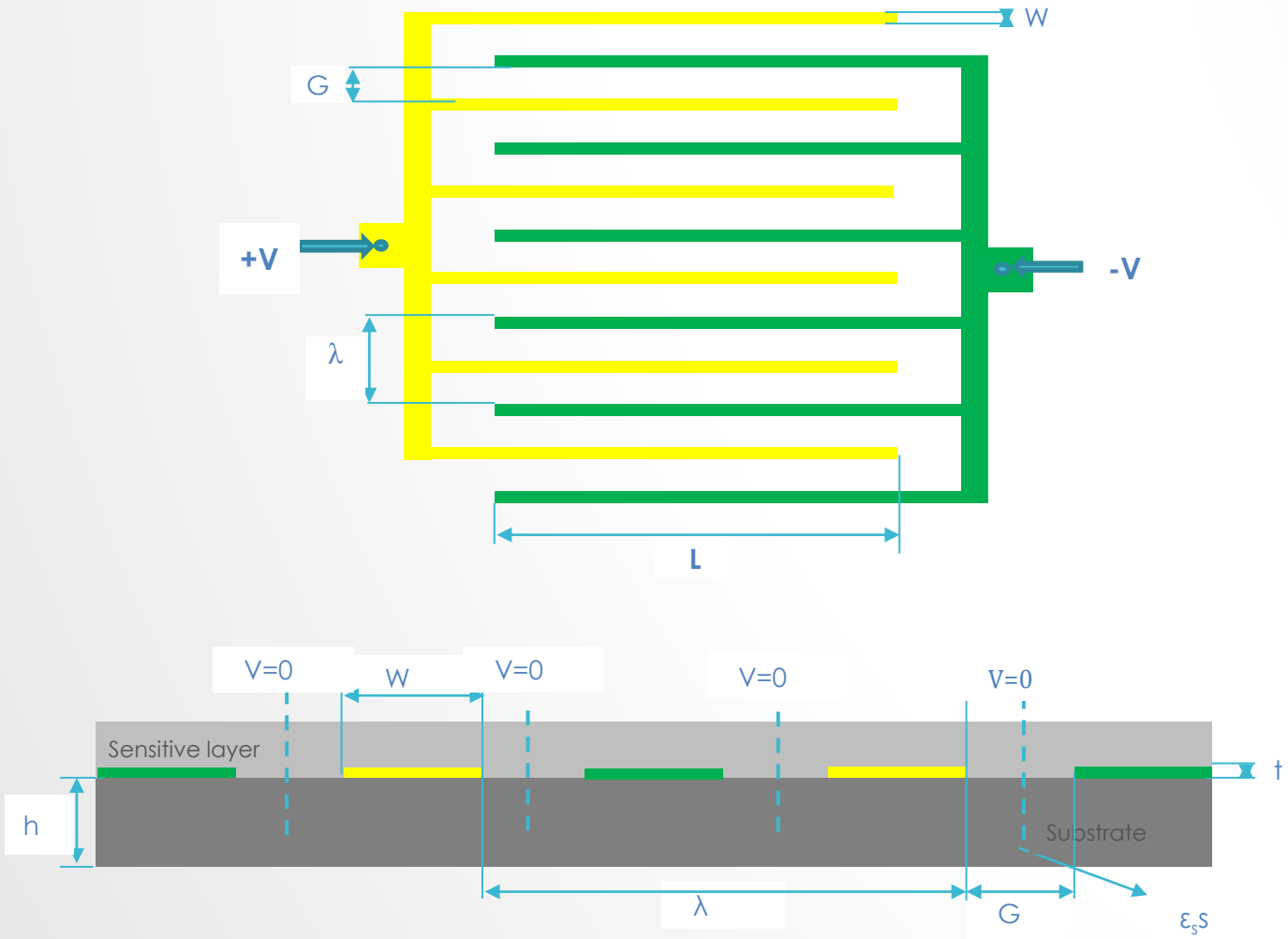

Fig. 1. (a) Layout of electrode plane; (b) Cross-section of a periodic IDC-S showing the electric potential boundary planes distribution.

By symmetry, the system geometry has an obvious property, which is helpful to divide the whole electrodes into a number of identical unit cells, of which dimension is λ/2, from the center of electrode to the mid-point of adjacent pole.

In a geometrically symmetrical capacitor, the perpendicular plane halfway between electrodes is equal-potential planes. In common this plane is considered as an electric ground and its voltage is set to zero. The electric field lines cross normal to this plane as shown in Fig. 2.

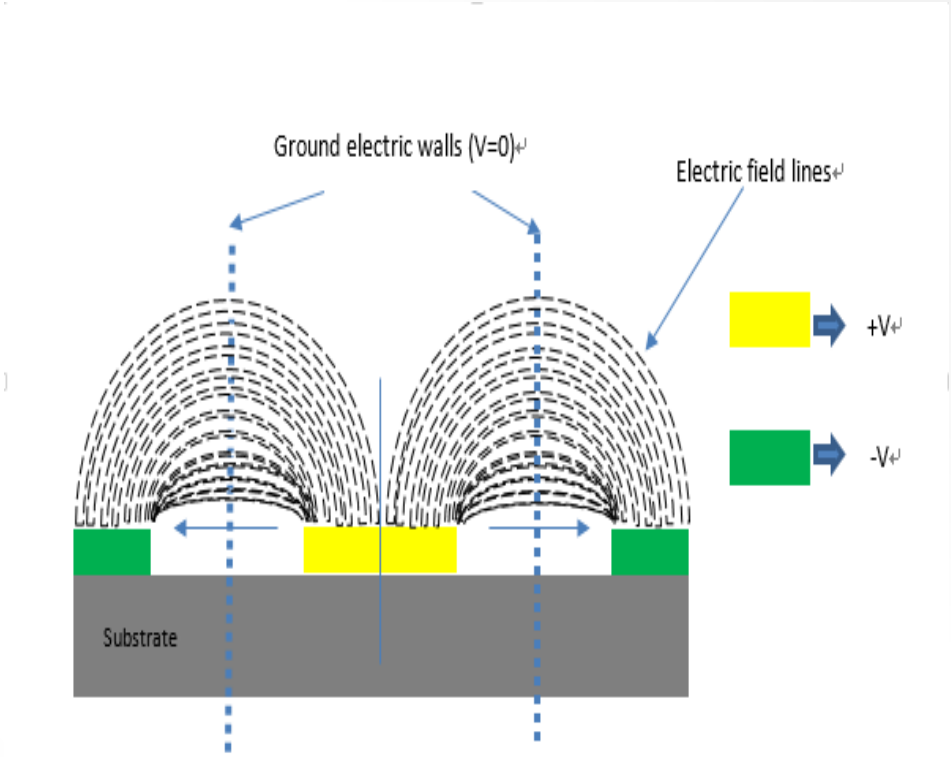

- **Fig. 2. Two Unit-cells model of the proposed multi-layered interdigital capacitor**

THEORY AND CALCULATION

Capacitance

1. Single semi-infinite layer capacitance

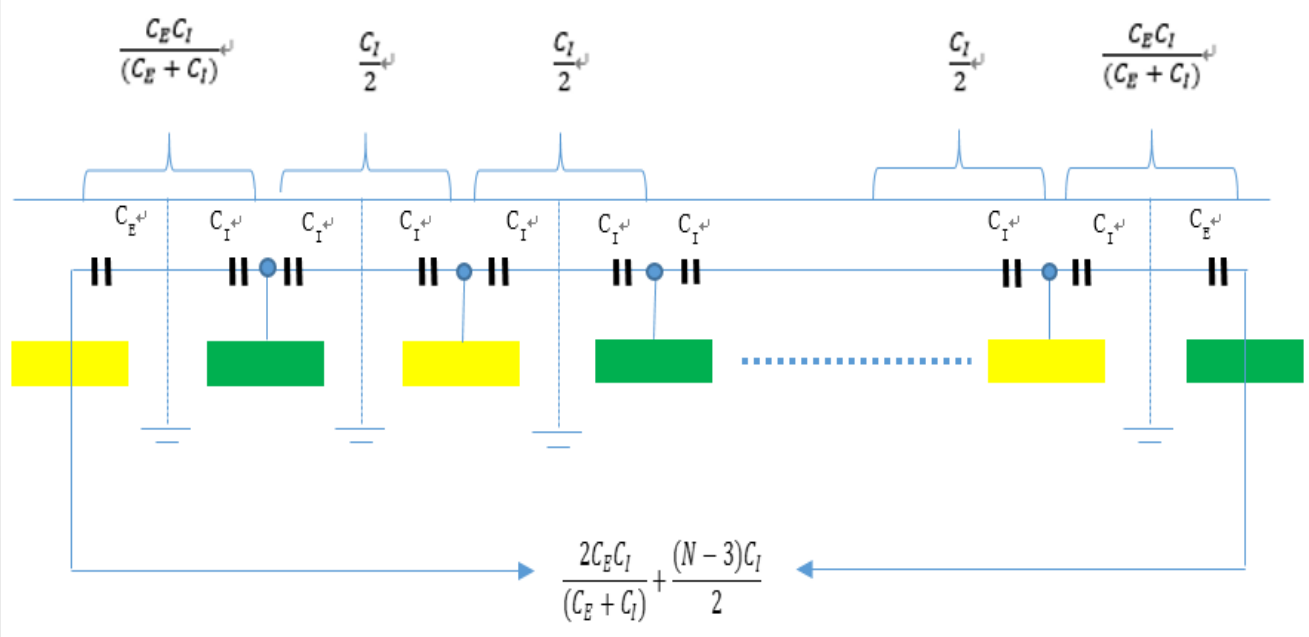

Fig. 4. Schematic of the equivalent circuit for evaluation of the static capacitance of a semi-infinite top layer in a periodic IDC-S with N electrodes.

As shown above figure, it is not hard to disclose that the total capacitance between positive and negative electrodes of a semi-infinite layer IDC-S is presented as below:

$$C= (N-3)*C_I/2+2C_1*C_E/ (C_1+C_E), \quad (1)$$

Where,

N ----- The number of electrodes.

C_I------The capacitance of one interior electrode relative to the ground potential.

$C_{E------}$ The capacitance of one outer electrode relative to the ground plane next to it.

On the other hand, we can figure out as the number of electrodes increases $C \approx (N - 1)/2*C_I$, so for many practical cases, we only need to calculate $C_{I.}$

2. N-layer capacitance

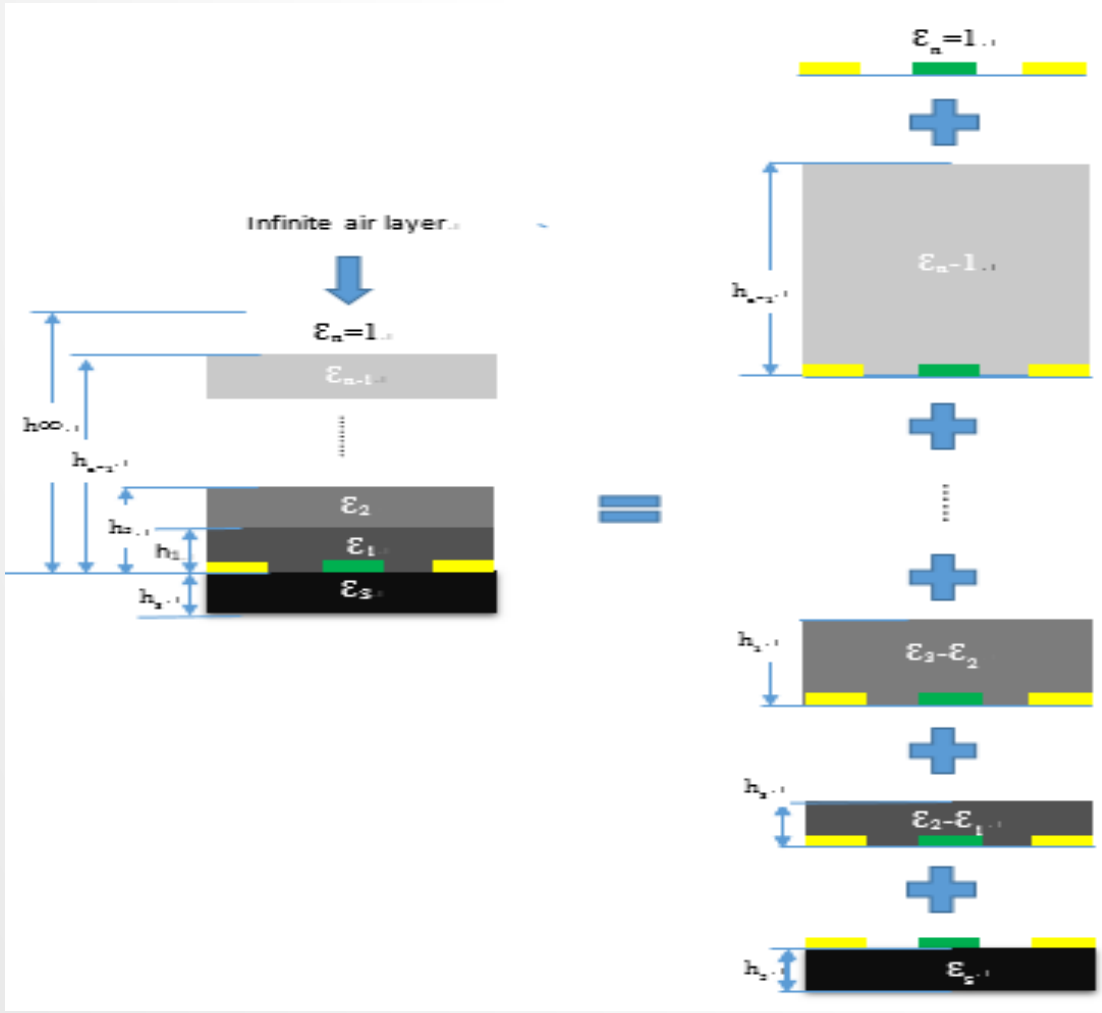

Fig. 5. Splitting of a N-layered plane according to the partial capacitance technique.

We can obtain

$$C_I = \sum_{i=1}^{n-1}(\varepsilon_i - \varepsilon_{i+1}) * C_I\,(h_i) + (\varepsilon_n + \varepsilon_S) * C_I(\infty)$$
$$C_E = \sum_{i=1}^{n-1}(\varepsilon_i - \varepsilon_{i+1}) * C_E\,(h_i) + (\varepsilon_n + \varepsilon_S) * C_E(\infty)$$

Where,

C_I ----- the interior capacitance of multi-layer plane.

C_E ----- the exterior capacitance of multi-layer plane.

C_h ----- the geometric capacitance of one layer, which depends on its height h and on the particular electrode geometry.

ε_i ----- the relative permittivity of the i^{th} layer.

ε_S ----- the permittivity of the inert substrate.

$C_I(h_i)$ ---- the geometric capacitance of i^{th} layer with height h_i for inner fingers.

$C_E(h_i)$ ---- the geometric capacitance of i^{th} layer with height h_i for outer fingers.

3. Computation of $C_I(h_i)$ and $C_E(h_i)$

a. λ=2(G +W) is the spatial wavelength,

b. η is the metal ratio between the electrode width and the unit cell width which is known as the metal ratio, and

c. r is the ratio between the thickness of each layer and the spatial wavelength

	Interior electrodes	Exterior electrodes
Finite layer	$C_I = \epsilon_0\epsilon_r \frac{\mathcal{K}(k_I)}{\mathcal{K}(k_I')}$	$C_E = \epsilon_0\epsilon_r \frac{\mathcal{K}(k_E)}{\mathcal{K}(k_E')}$
	$k_I' = \sqrt{1-k_I^2}$	$k_E' = \sqrt{1-k_E^2}$
	$k_I = t_2\sqrt{\frac{t_4^2-1}{t_4^2-t_2^2}}$	$k_E = \frac{1}{t_3}\sqrt{\frac{t_4^2-t_3^2}{t_4^2-1}}$
	$t_2 = sn(\mathcal{K}(k)\eta, k)$	$t_3 = \cosh(\frac{\pi(1-\eta)}{8r})$
	$t_4 = \frac{1}{k}$	$t_4 = \cosh(\frac{\pi(1+\eta)}{8r})$
	$k = \sqrt{\frac{v_2(0,q)}{v_3(0,q)}}$	$\eta = \frac{g_C}{g_C + w_C} = \frac{2g_C}{\lambda}$
	$q = e^{-4r\pi}$	$r = \frac{h}{\lambda}$
Infinite layer	$C_I = \epsilon_0\epsilon_r \frac{\mathcal{K}(k_{I\infty})}{\mathcal{K}(k_{I\infty}')}$	$C_E = \epsilon_0\epsilon_r \frac{\mathcal{K}(k_{E\infty})}{\mathcal{K}(k_{E\infty}')}$
	$k_{I\infty} = \sin(\frac{\pi}{2}\eta)$	$k_{E\infty} = \sin(\frac{2\sqrt{\eta}}{1+\eta})$

Inductance

The entire inductance of the parallel wires is calculated using Eq.

$$L_{coil} = \frac{1}{\sum_{i=1}^{n} L_{wire,i}^{-1}}$$

In general the inductance of a wire i, Lwire,i is given by the sum of self-inductance Ls,i of mutual inductance Lm,i

$$L_{wire,i} = L_{s,i} + L_{m,i}$$

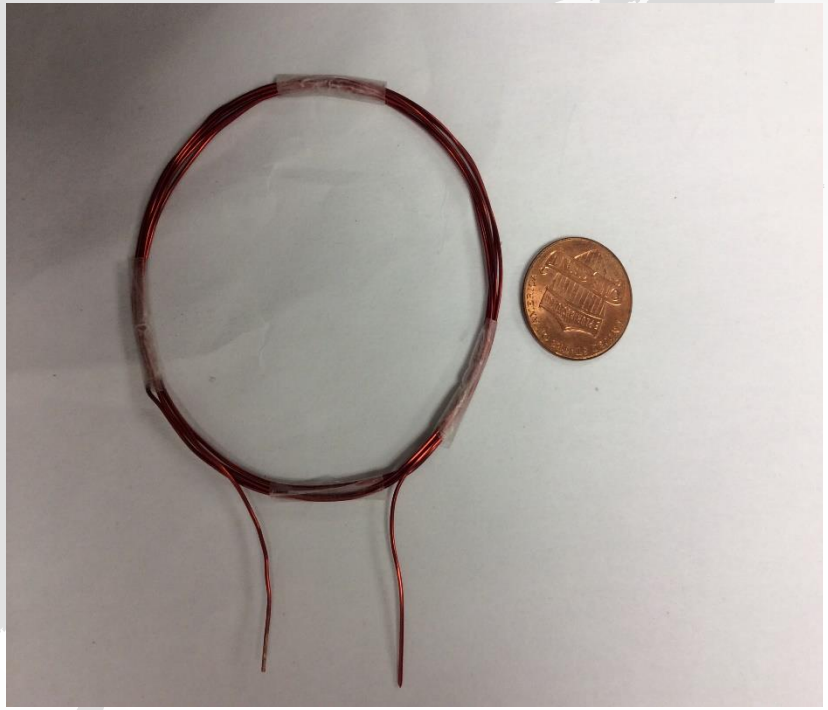

Resonant Frequency

A general resonant circuit is comprised of elements that dissipate energy and store energy: resistive components dissipate energy and reactive components store energy. Stored energy gives rise to a phase shift between the voltages and currents in a system. A positive value of reactance is defined as inductive and a negative value of reactance is defined as capacitive.

The expression of the resonant frequency is given by the following equation:

$$f_r = \frac{1}{2\pi\sqrt{L_S C_S}}$$

SENSOR DESIGN AND OPTIMIZATION

DNA Sensing Principles.

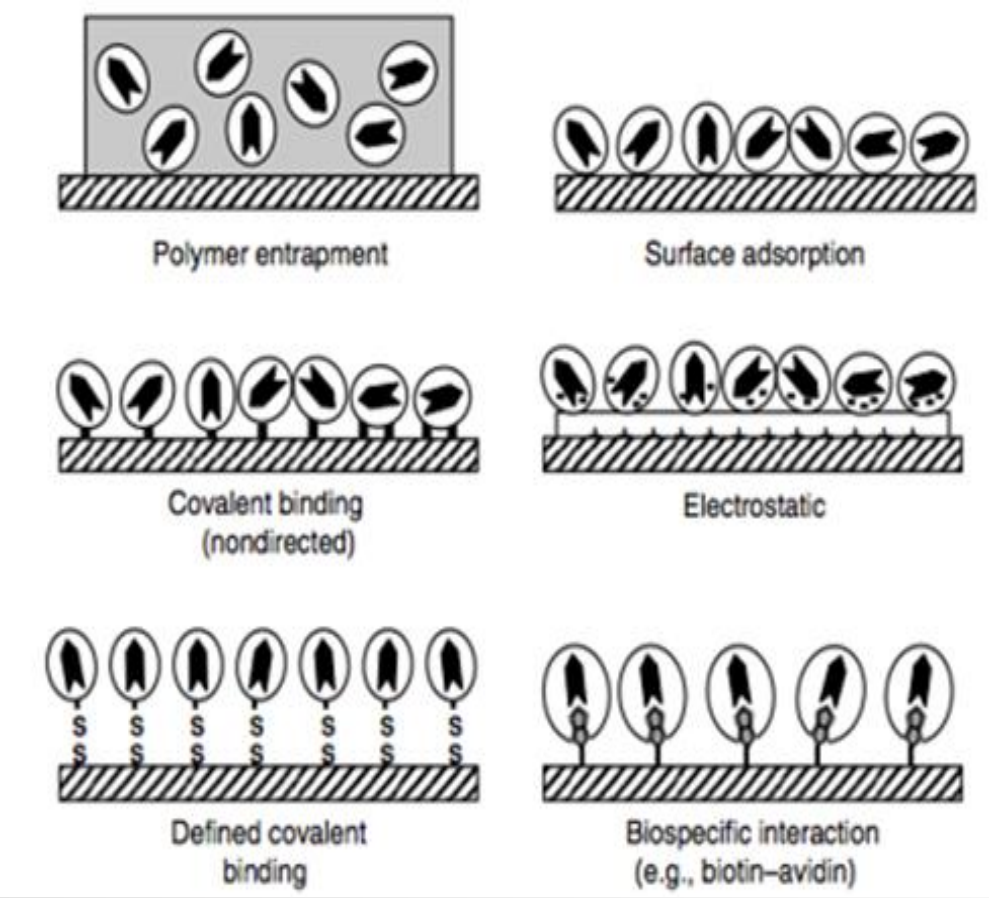

Fig 6 Methods for immobilizing different biomolecules onto electrode surfaces

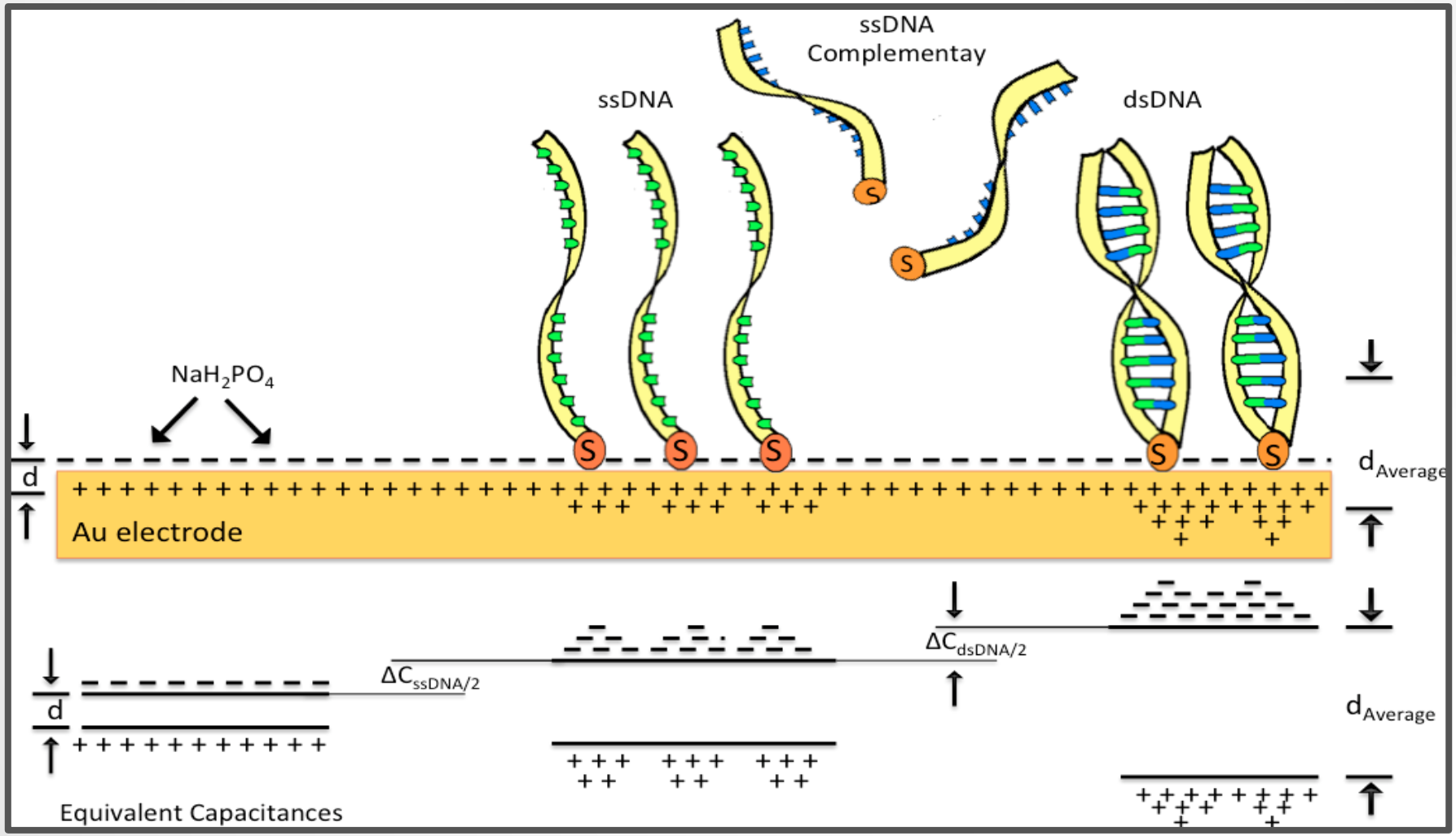

Fig. 7 Tendency of the equivalent capacitances for DNA immobilization and hybridization

Optimization of capacitor design.

From previous section, we obtain:

$$C=C(\eta, r, \varepsilon_r, N, L, \varepsilon_S).$$

a. W_1=10μm, G_1=5μm, L=2mm, N=130; ⇒ η=0.667 λ=30μm

b. W_2=10μm, G_2=10μm, L=2mm, N=130; ⇒ η=0.5 λ=40μm

c. W_3=5μm, G_3=5μm, L=2mm, N=130. ⇒ η=0.5 λ=20μm

1. IDC-S with top air layer

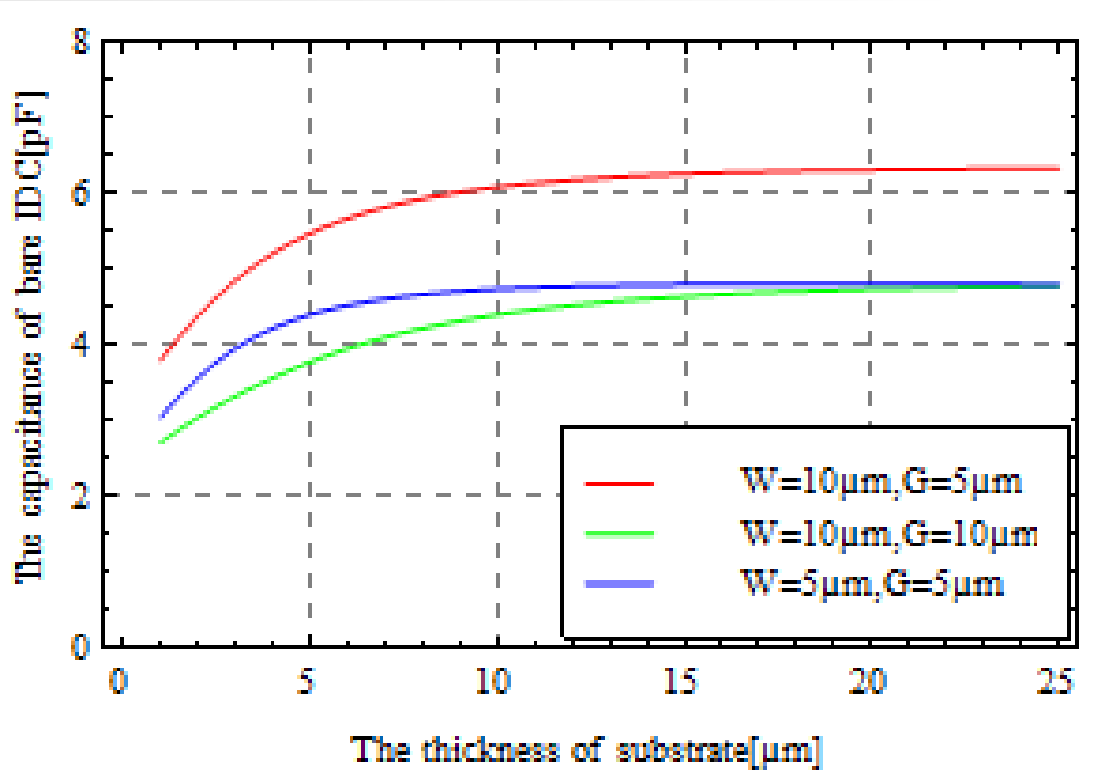

Fig. 8 Dependence of capacitance on h_s

Assume that the substrate permittivity. (ε_S=3.15)

$$h_s \geq r_{saturated} * \lambda$$

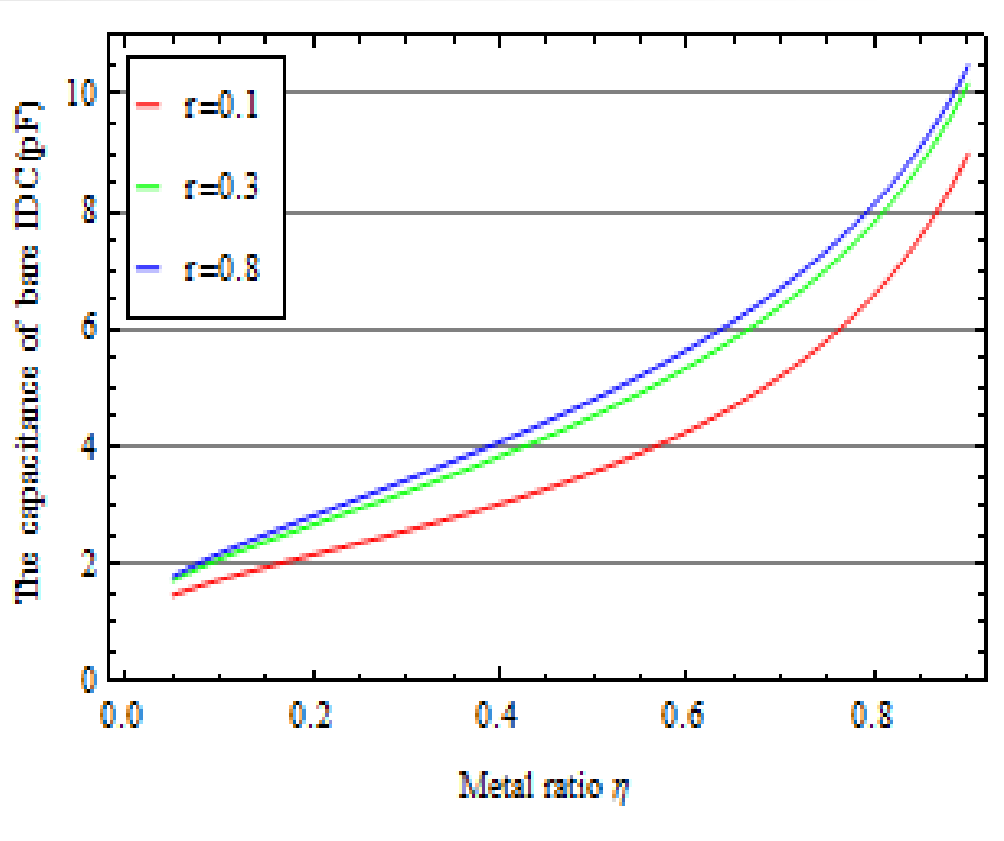

Fig. 9 Dependence of capacitance on η

As noticed in the range 0.9 and more of η the change of capacitance is nonlinear. Thus, in order to have a better sensing linearity, in real design, we are trying to avoid this range.

2. IDC-S with one sensitive layer

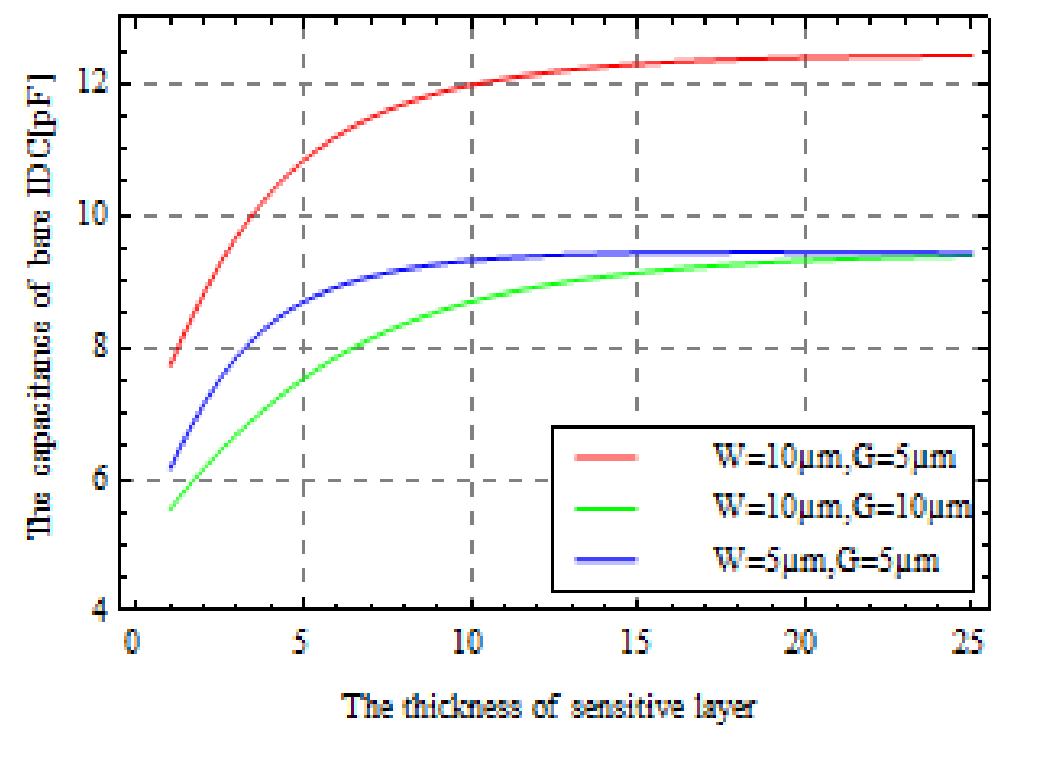

Fig. 10 Dependence of capacitance on h_s

The simulation parameters are as follows: ε_r=5; ε_s=3.15; N=130; L=2mm.

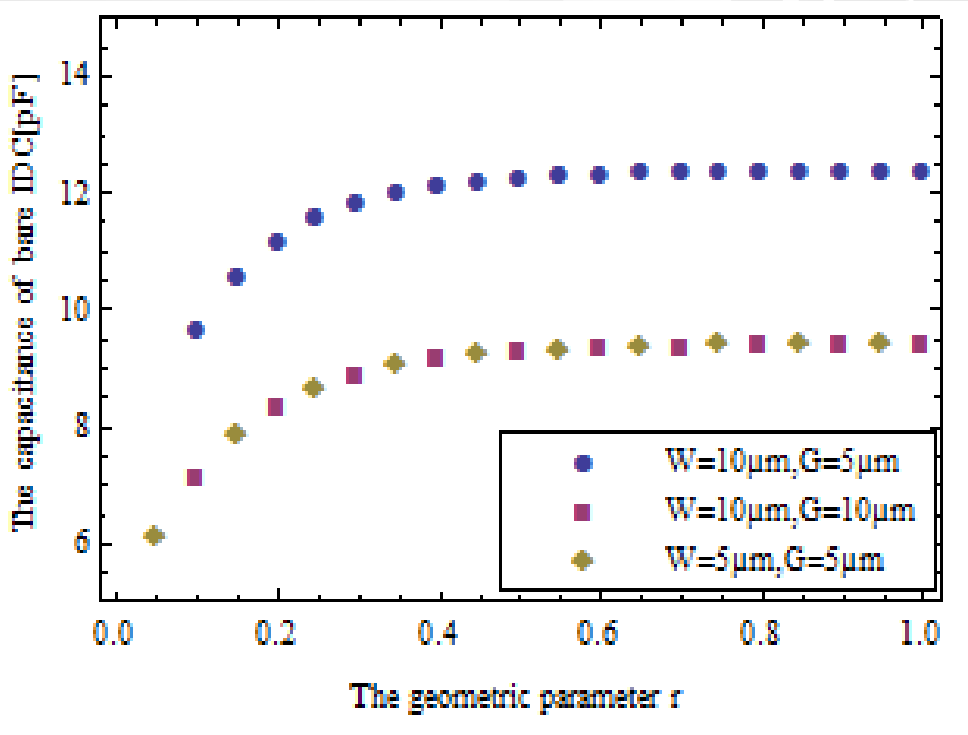

Fig. 11 Dependence of capacitance on geometric parameter r

If r is larger than its saturated value, no matter what great change it has on the electrodes, we only get a constant capacitance.

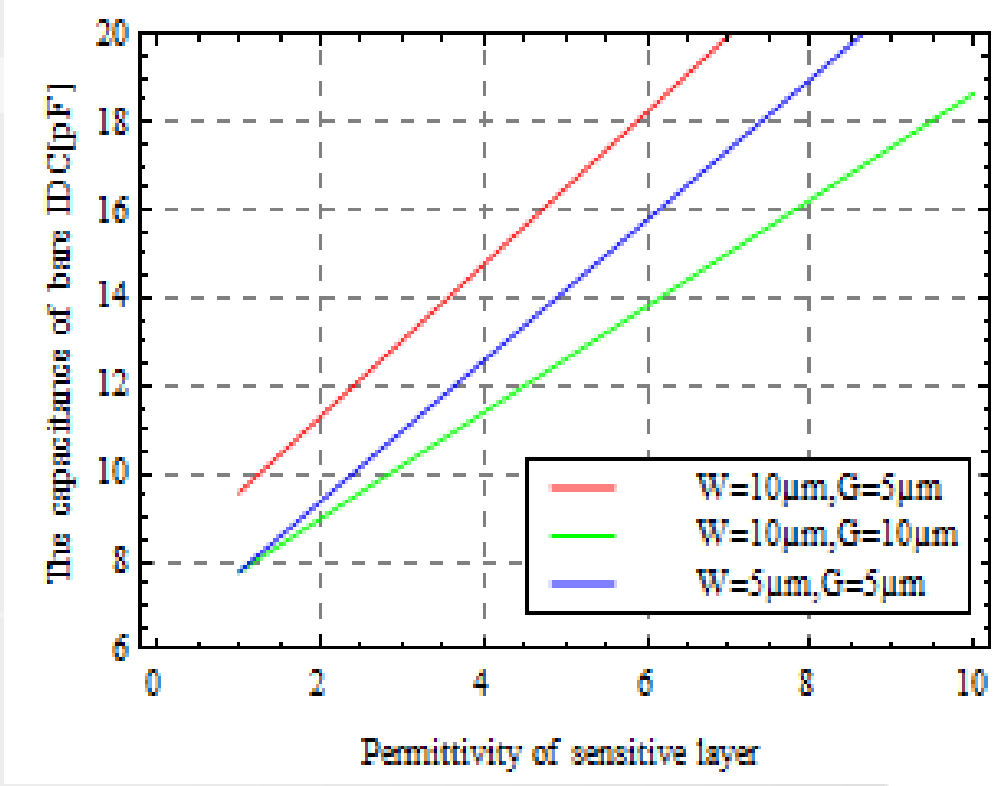

Fig. 12 Dependence of capacitance on permittivity of sensitive layer

SENSOR CHARACTERIZATIONS

Equipment and Instrumentation

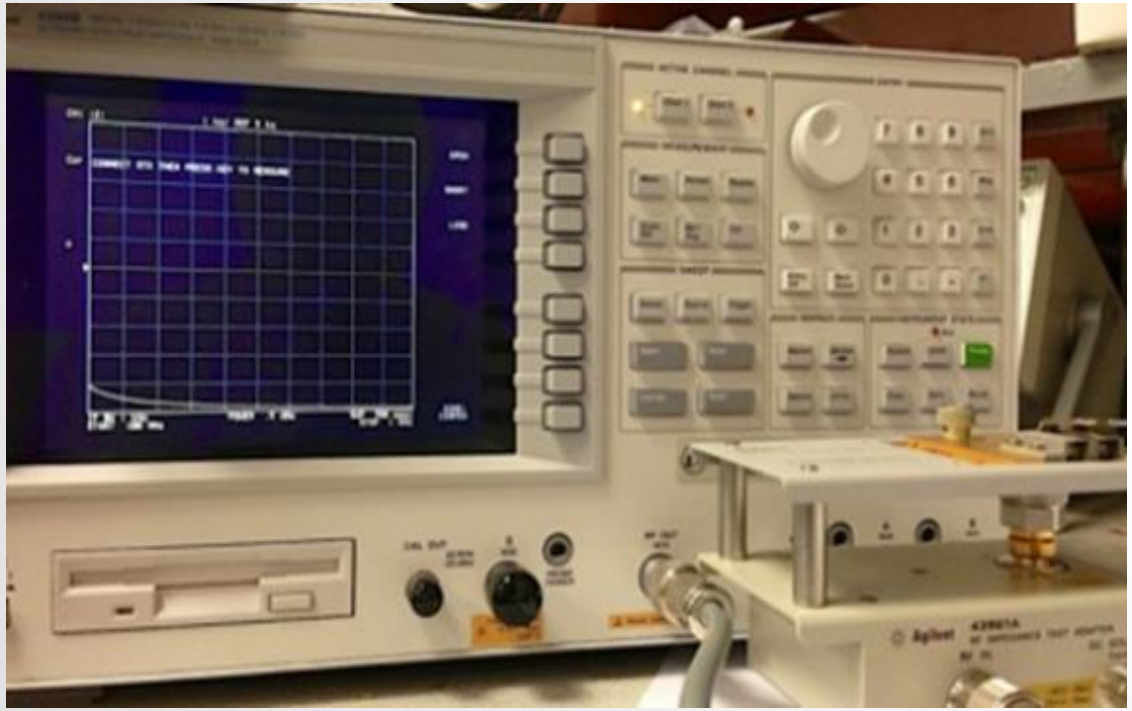

Fig 17 Agilent 4396B setup with impedance test kit Agilent 43961A

Agilent 4396B Impedance Analyzer and the impedance test kit 43961A are used to measure impedance and frequency (Fig. 17). This equipment working in a frequency range of 100 kHz to 1.8 GHz can be used to measure the sensor sensitivity with a wireless measurement technique.

Fig 18 **Agilent 4285A** Precision LCR meter

On the other hand, for capacitance measurement, a precision LCR meter, the Agilent 4285A (Fig. 18) that works on a frequency range of 75 kHz to 30 MHz is applied to measure the sensor sensitivity directly with a specific home-made fixture.

Experiment Setup

1. Dummy Test

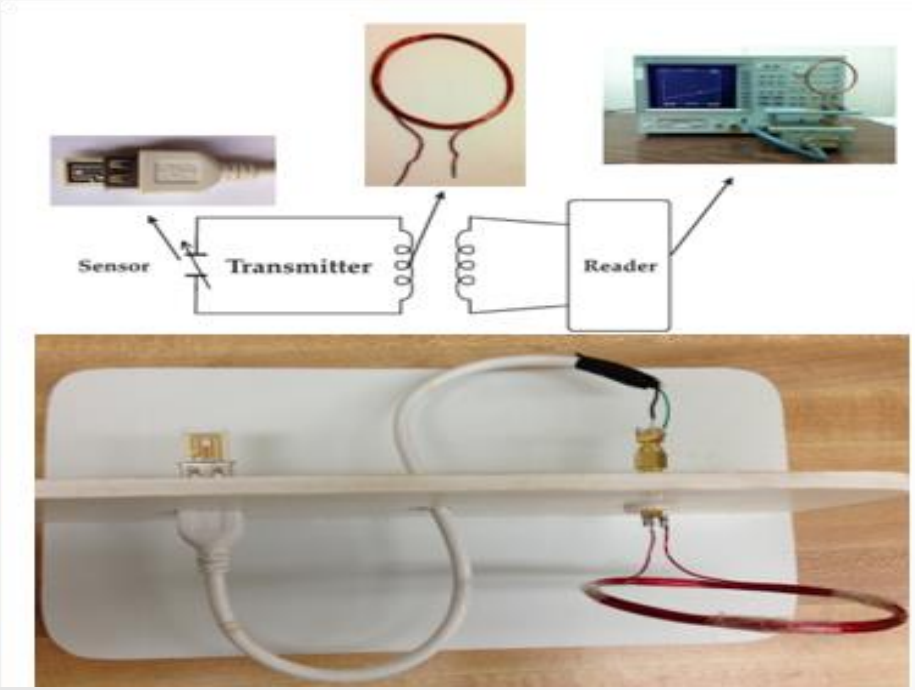

Fig 19 Impedance test antenna arrangement

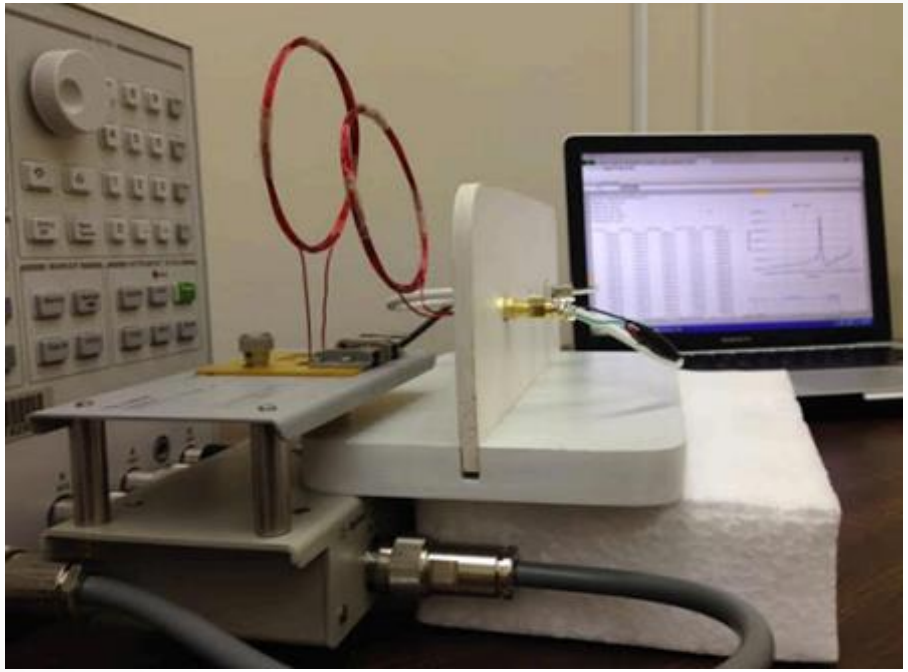

Fig 20 Experimental setup

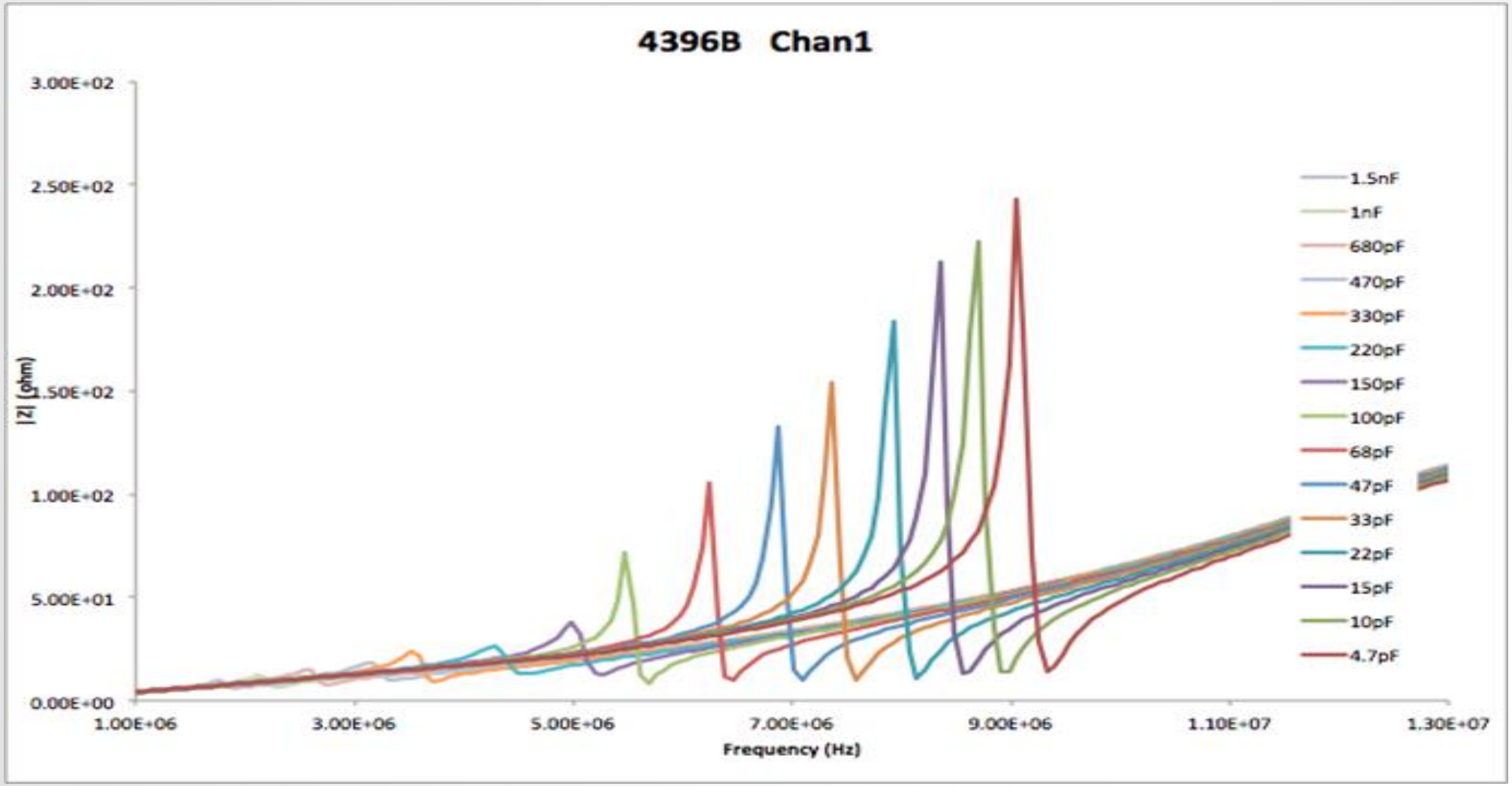

Fig 21 The resonant frequency versus the known-value capacitance

2. Actual Measuring Test Setup

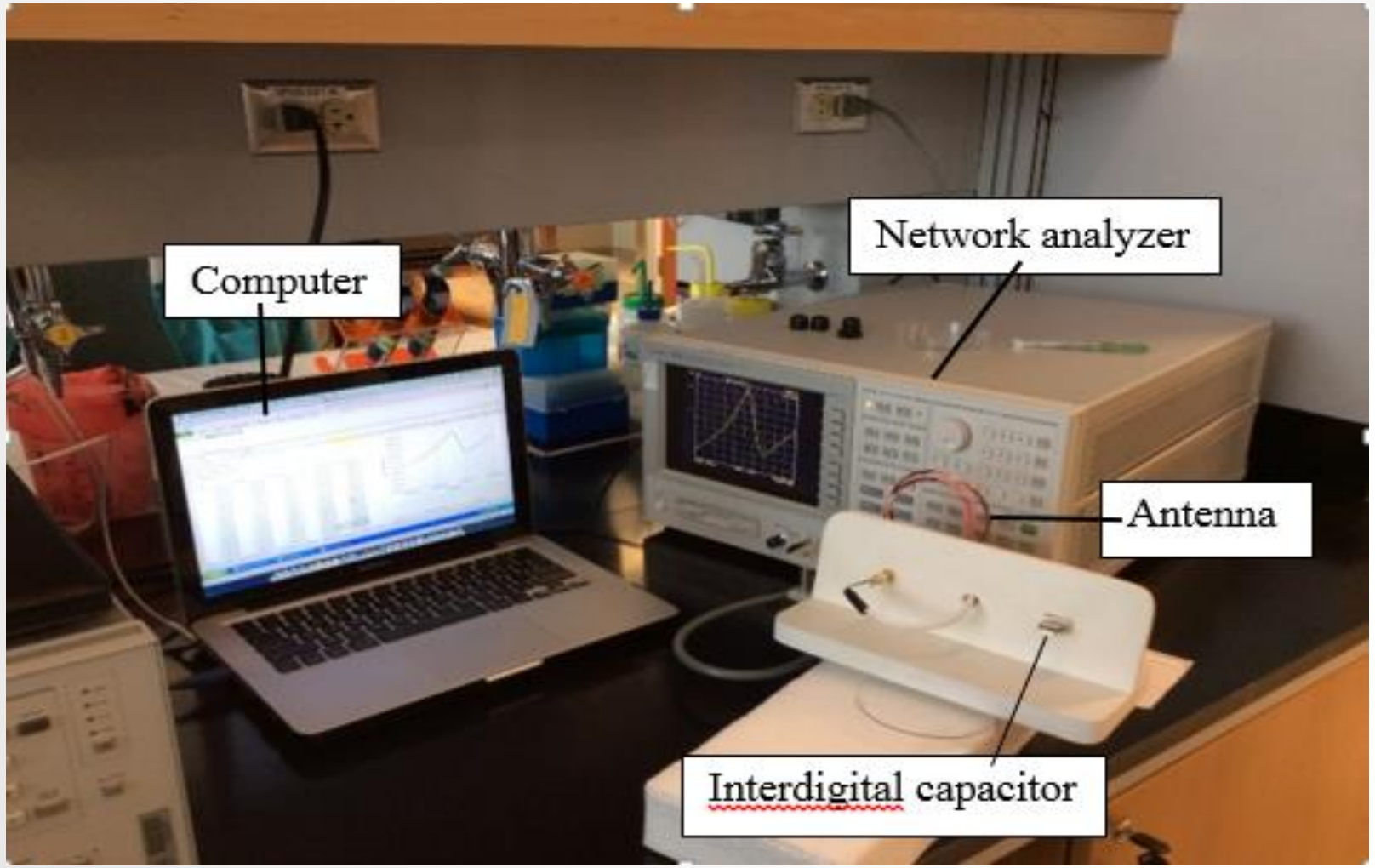

Fig 22 Sensor calibration setup with network analyzer

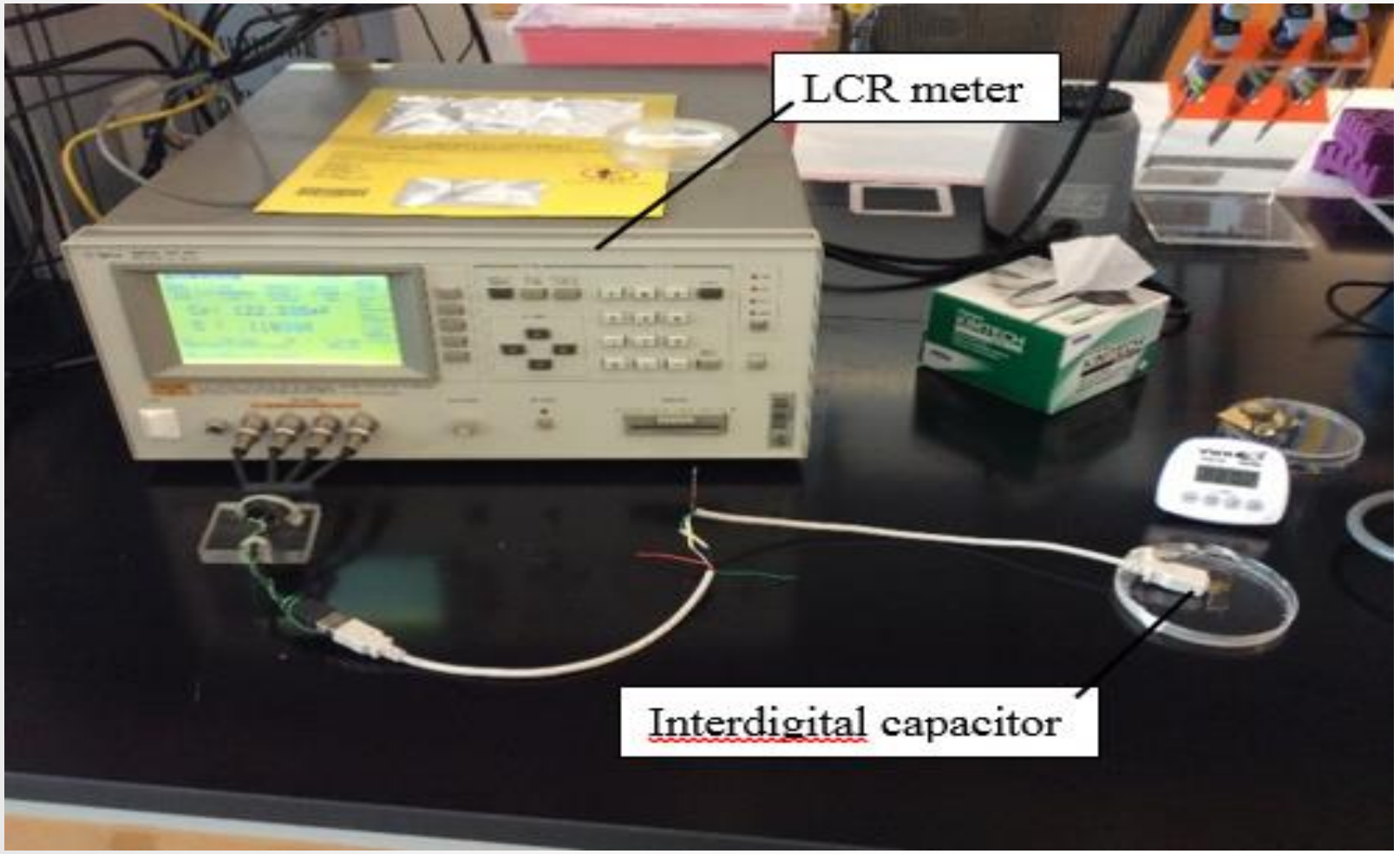

Fig 23 Sensor calibration setup with LCR meter

Sensor Performances Characterization

1. Experiment Procedure

Step 1 Calibration: the Open, Short, and 50 Ω terminations in the calibration kit are required. In respect to LCR meter, the open and short circuit test were performed leaving an open or short connection between the IDC connection station docking.

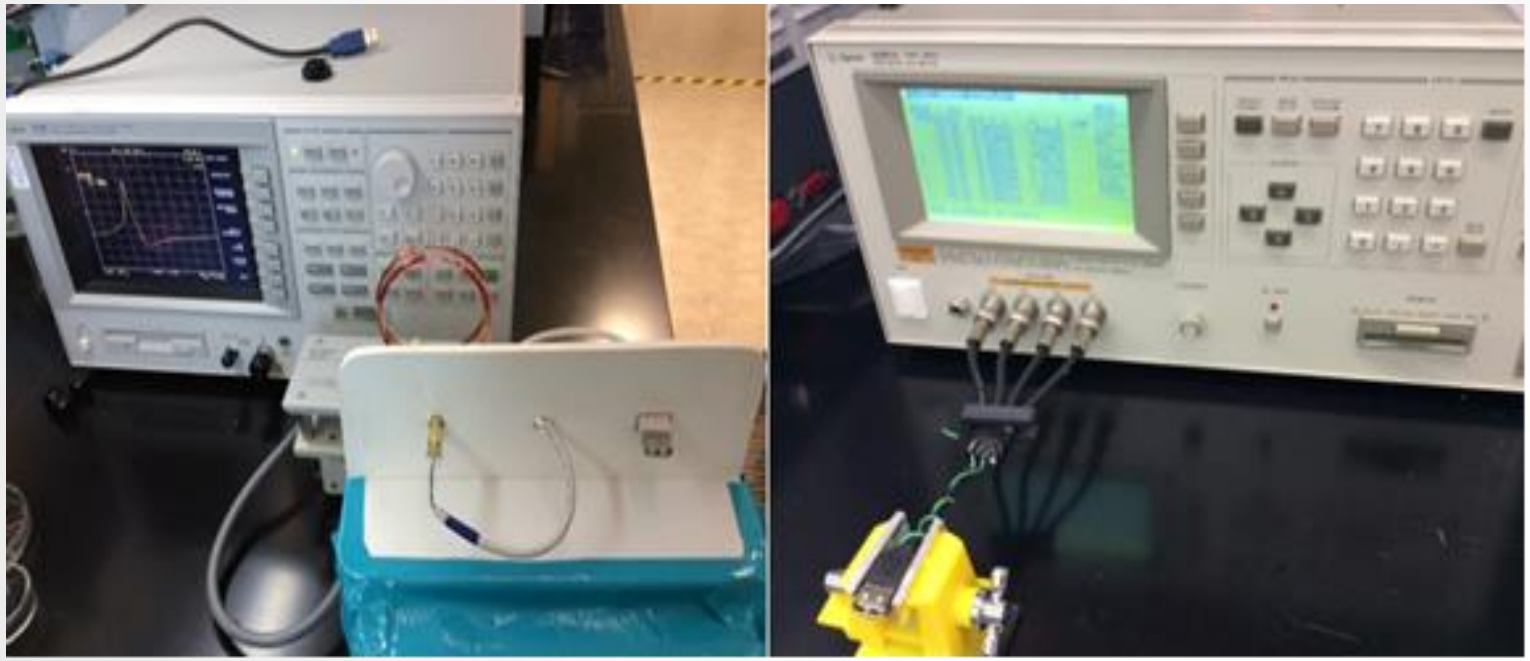

Fig 24 Baseline measurement

Step 2 Baseline measurement: The value of frequency peak is measured and recorded without proposed sensor involved. The measurement is designed to demonstrate the resonant frequency change with or without IDC.

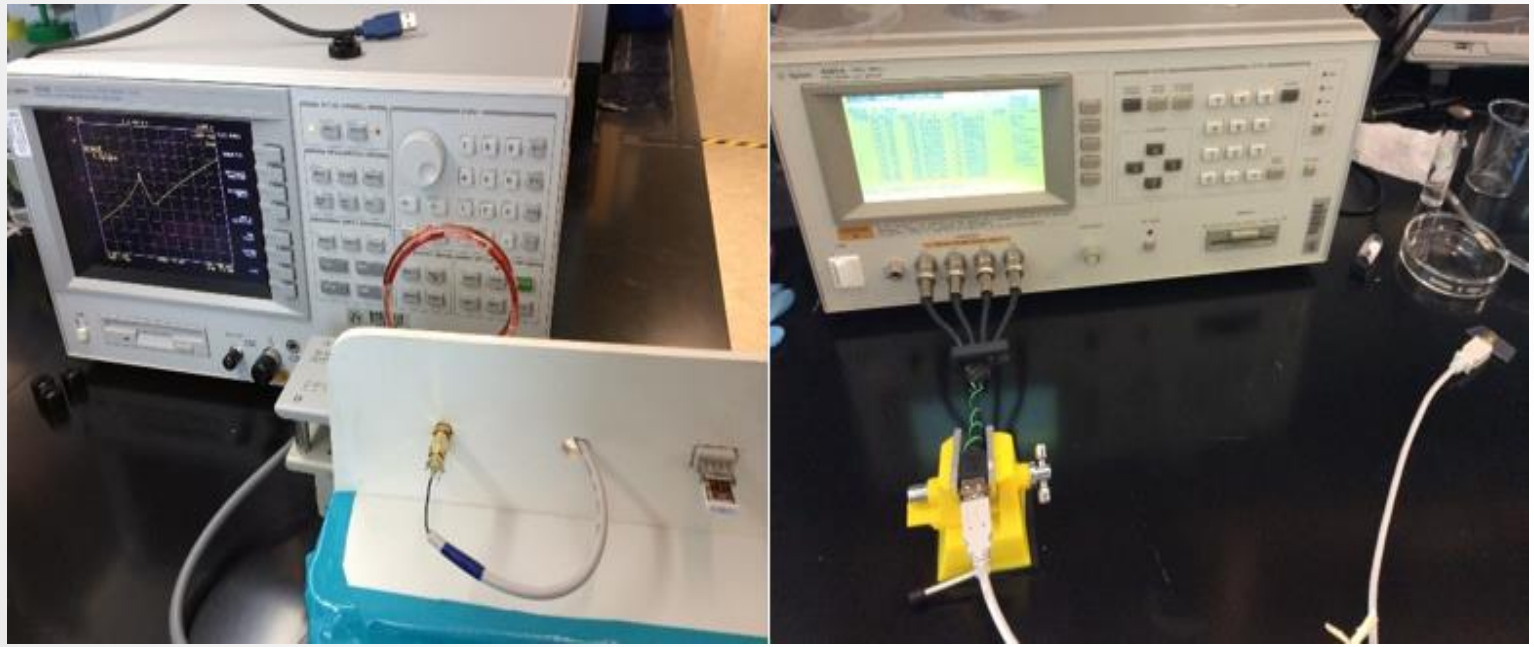

Fig 25 Measurement with bare electrodes

Step 3 Measurement with bare electrodes: The curve peak moved to left in response to IDC plugged into female USB port. For direct capacitance measurement, the value of capacitance increased.

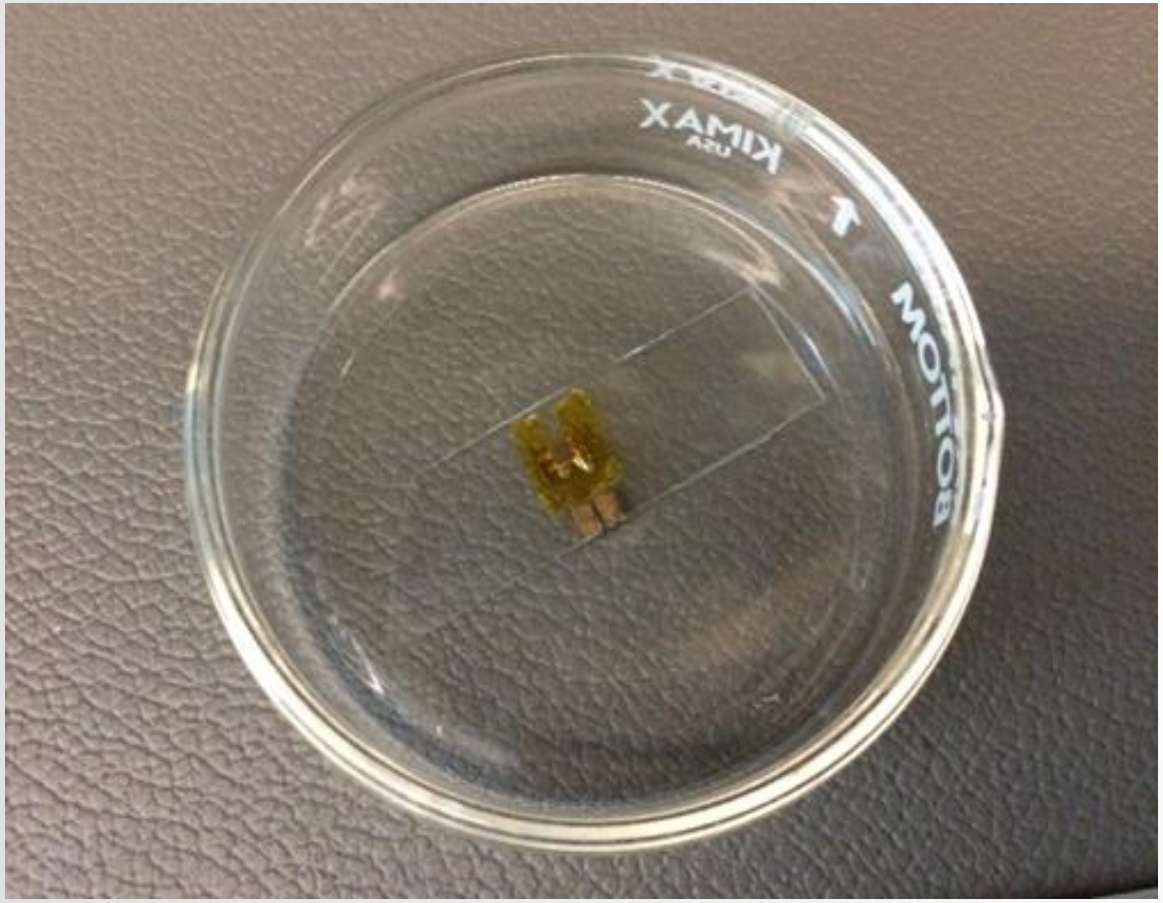

Fig 26 Preparation of ssDNA for immobilization

Step 4 Measurement of ssDNA: Drop of 5 mM ssDNA solution was deposited on the interdigital part enclosed by insulated tape to prevent connection between positive and negative electrodes causing short circuit, then kept in a clean dish for 20 hours. After that, the electrode was rinsed with specific buffer and dried with a nitrogen stream for removing the excess unattached to electrodes. Finally, the frequency peak is observed by network analyzer. Also, the capacitance can be obtained by LCR meter readout.

Step 5 Measurement of 5mM ssDNA with non-complementary target: After ssDNA molecule was immobilized to electrode surface, non-complementary strand of DNA is introduced and dropped. The cleaning with buffer and nitrogen would be done in 3 hours later and following measurement was taken. The measurement is aimed at being a blank experiment for DNA hybridization process.

Step 6 Measurement of 5mM ssDNA with complementary target: Repeat step 5 with adding complementary strand of DNA instead of the non-complementary one. This step would also take 3 hour and same cleaning task before measurement.

2. Experiment Result

2.1 Clean IDAM capacitance Result

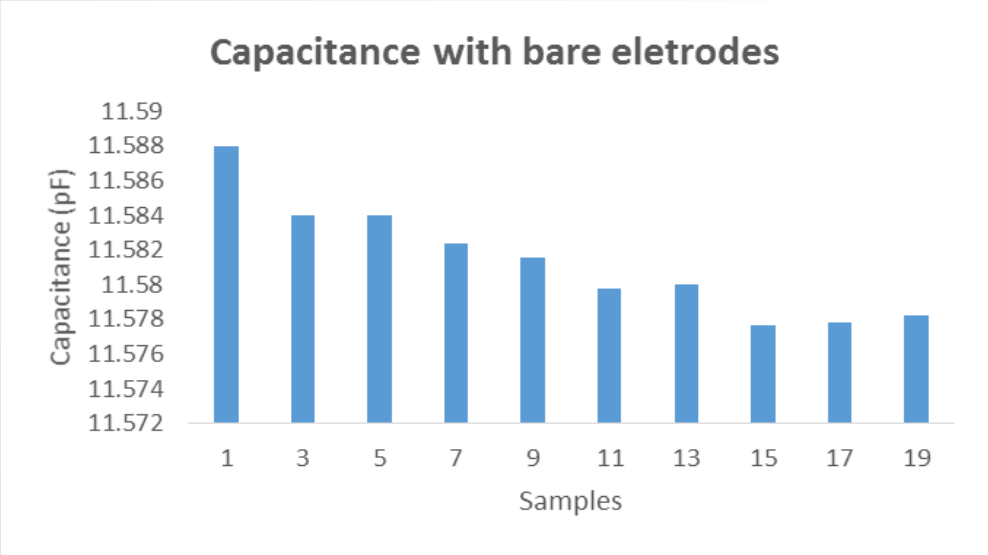

Fig 27 Clean IDAM capacitance in air

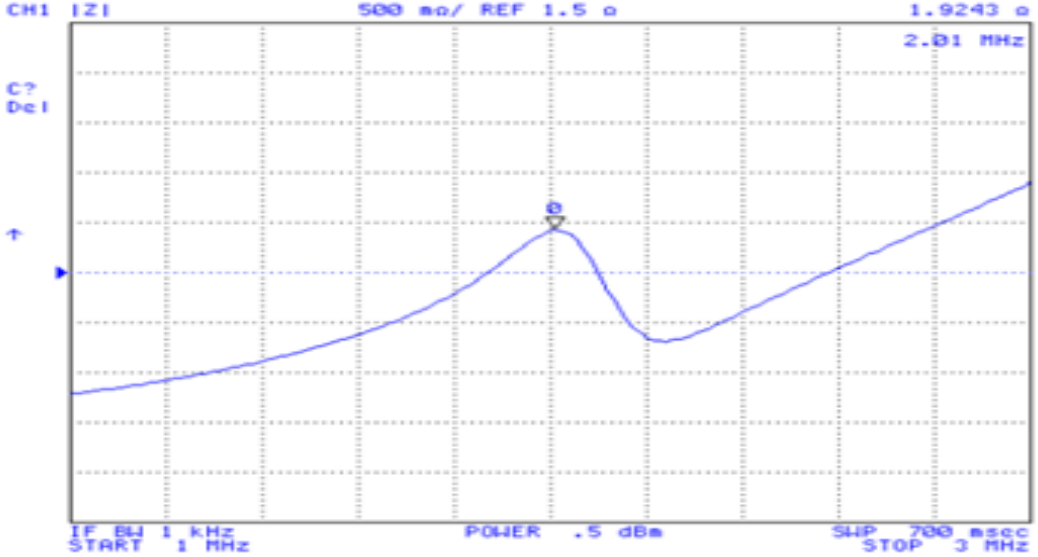

Fig 28 The impedance of bare clean electrodes

2.2 ssDNA immobilization

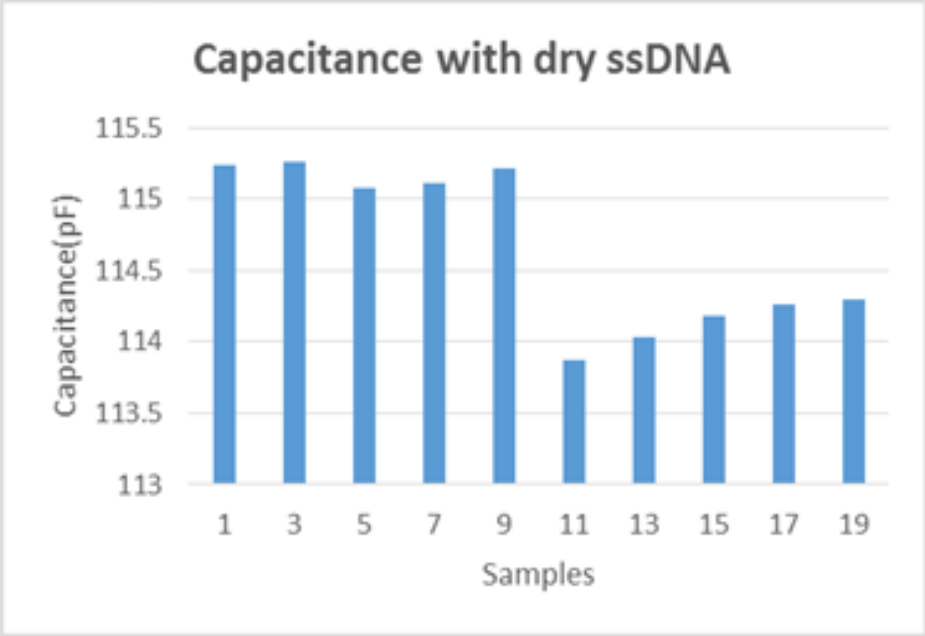

Fig 29 IDAM capacitance after ssDNA immobilization.

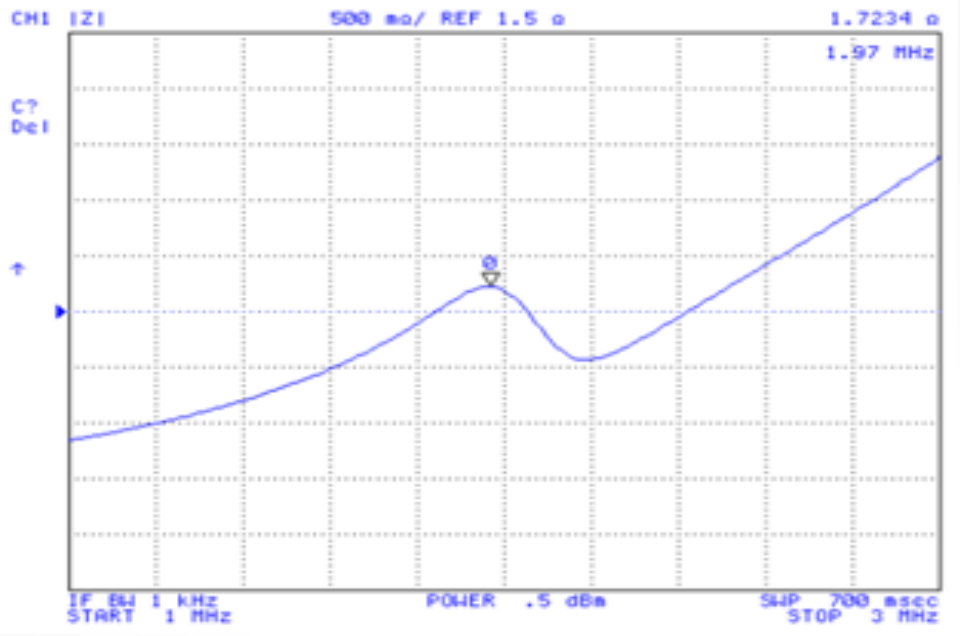

Fig 30 The impedance measurement after ssDNA immobilization

2.3 Hybridization of the Complementary Strand

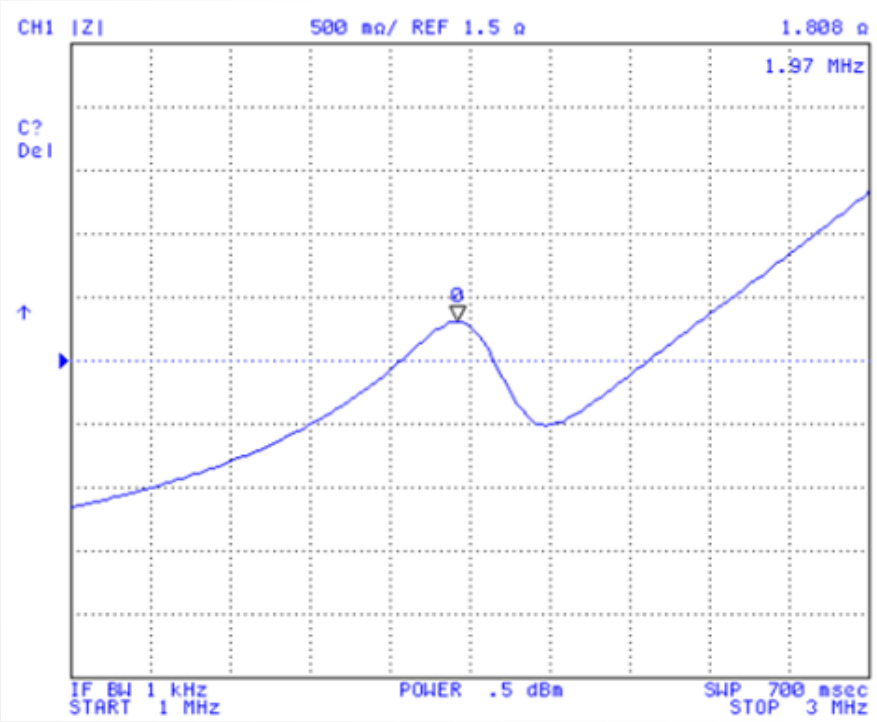

Fig 31 The impedance measurement after non-complementary strand

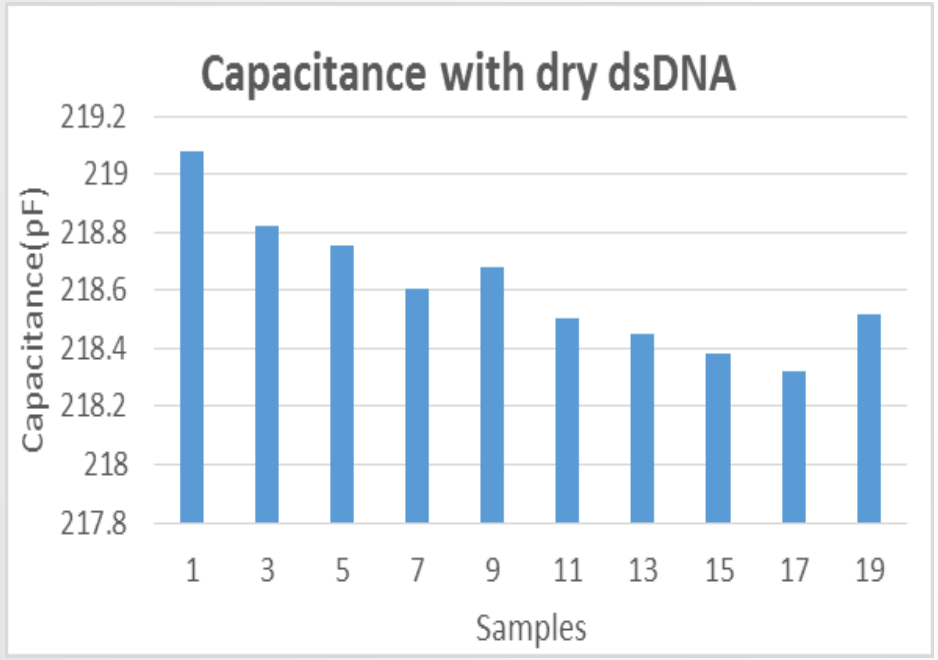

Fig 32 IDAM capacitance after dsDNA hybridization

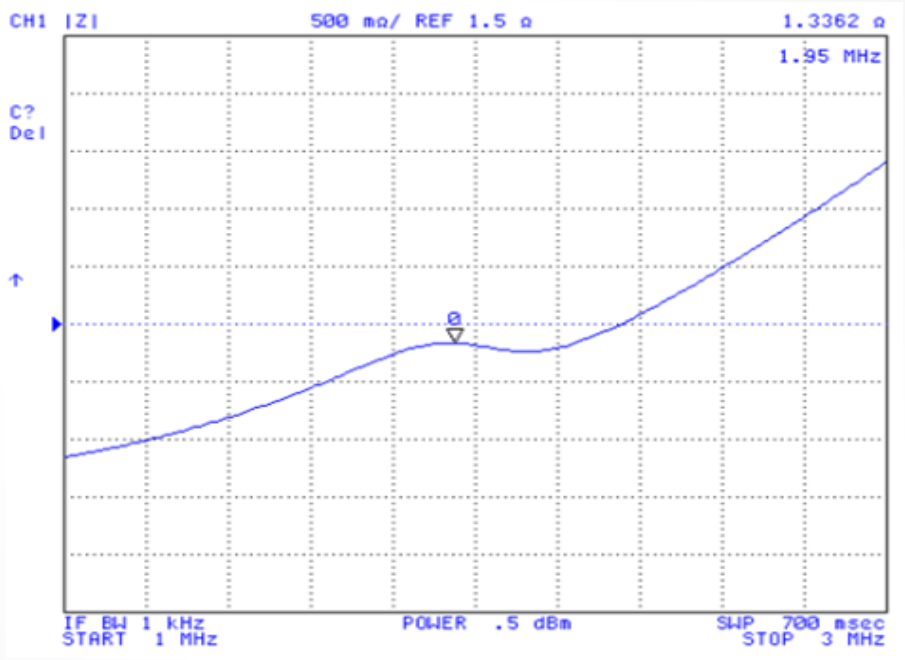

Fig 33 The impedance measurement after complementary strand

3. Result Analysis

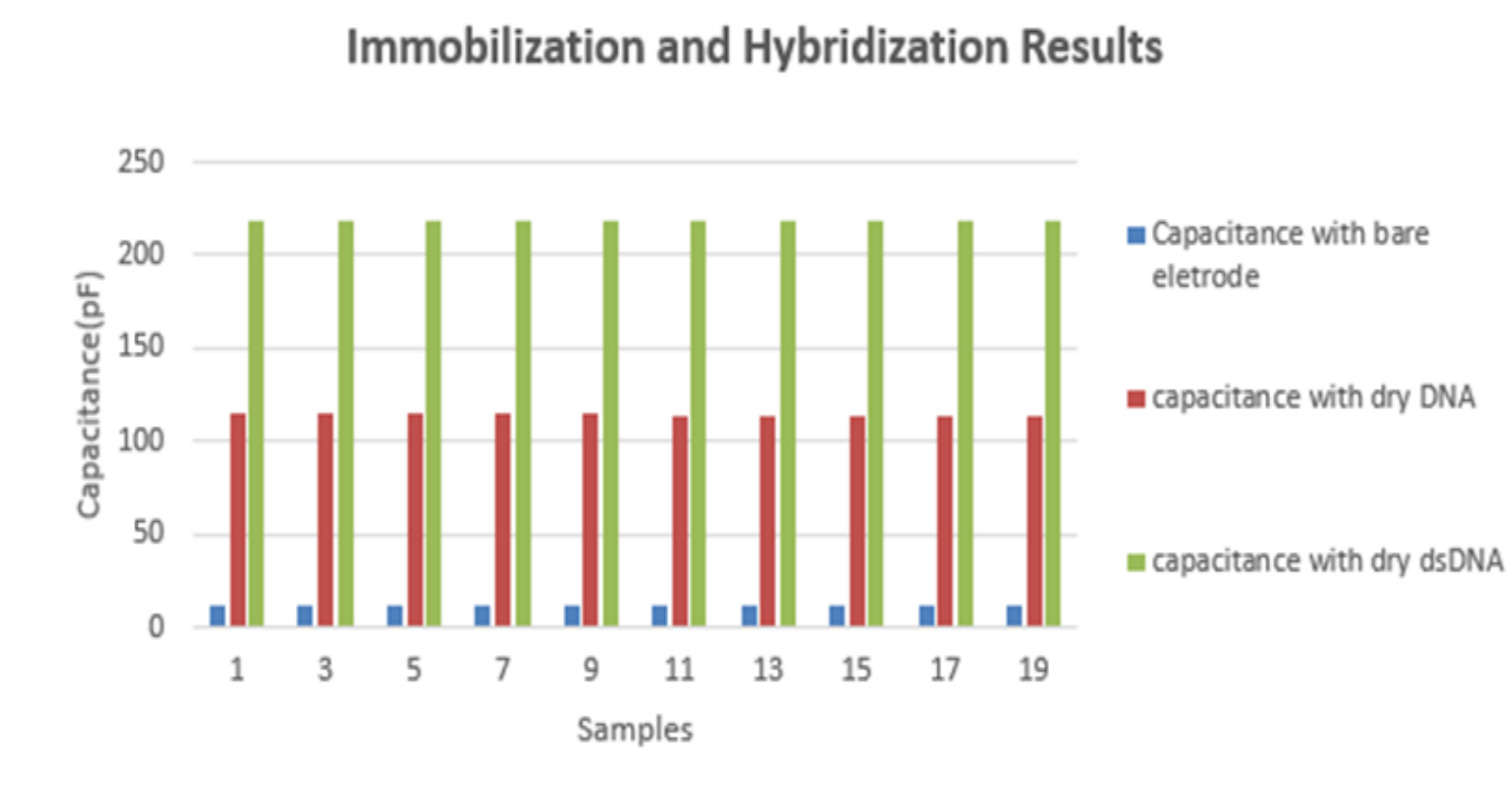

Fig 34 The average capacitance measurement after each experiment stage

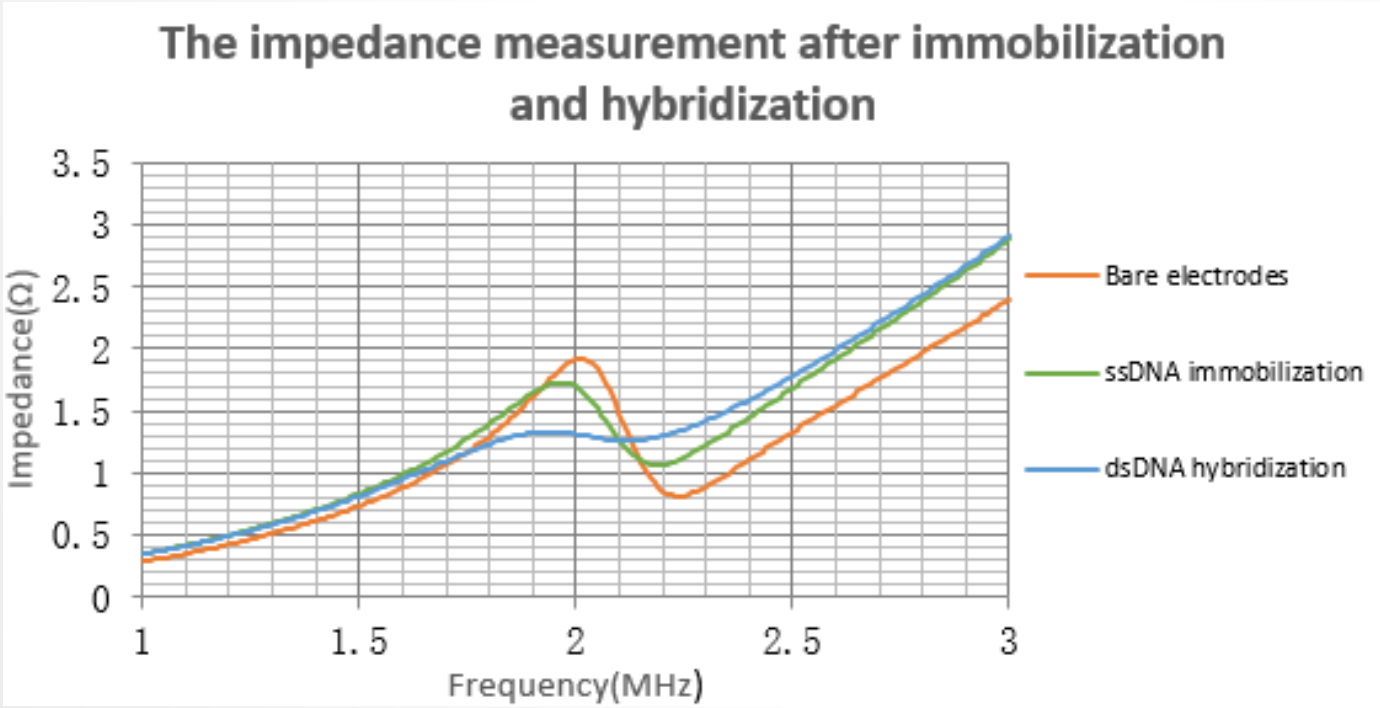

Fig 35 The impedance measurement after each experiment stage

Fig. 34 shows the capacitance increase after the immobilization and hybridization stage and the frequency peak decrease meanwhile as presented in Fig. 35. It is noticeable that each data point represents the average of 32 subsamples.

CONCLUSIONS AND FUTURE WORK

Conclusion

This research project has developed a novel passive wireless DNA molecule sensor, which has the structure with two major parts: a capacitor which is a DNA sensing element and an inductor which works as a passive power source and data communication element. These two components work together as an LC circuit, whose resonant frequency shifts when the capacitance of the sensor changes in response to DNA molecule behavior, to realize the wireless passive DNA sensing.

Following the analysis of every geometric factor of LC circuit based on capacitance and inductance modeling and simulation, optimized the sensor configuration was proposed and considerations of design were taken into account. The sensor prototype was then successfully fabricated to prove the concept of a DNA sensing device using passive wireless communication. Moreover, the experiment setup and biological methodology was indicated. Finally, sensor performance was analyzed and the experimental results paving the way for future work were demonstrated.

Future work

- Improve the IDC DNA sensor with higher sensitivity, linearity and minimized sensor size;
- Extend the communication distance of the DNA sensor;
- Develop a cost-effective way to read out the data transformed from proposed LC circuit, such as applying RFID technology;
- Investigate the DNA molecule experiment without limit of specific DNA sequence and molecule concentration;
- Attempt to figure out a time-saving method to treat the DNA molecule and accelerate DNA immobilization and hybridization.

References

[1] Ortiz, P., Jia, Y., Vargas, N. and Cabrera, C. (2013). Label-free capacitance DNA sensing. 2013 Seventh International Conference on Sensing Technology (ICST), Wellington, New Zealand.

[2] Millan, K. and Mikkelsen, S. (1993). Sequence-selective biosensor for DNA based on electroactive hybridization indicators. Analytical chemistry, 65(17), pp.2317-2323.

[3] Daniels, J. and Pourmand, N. (2007). Label-Free Impedance Biosensors: Opportunities and Challenges. Electroanalysis, 19(12), pp.1239-1257.

[4] Clausen-Schaumann, H., Rief, M., Tolksdorf, C. and Gaub, H. (2000). Mechanical stability of single DNA molecules. Biophysical Journal, 78(4), pp.1997-2007.

[5] Lao, R., Song, S., Wu, H., Wang, L., Zhang, Z., He, L. and Fan, C. (2005). Electrochemical interrogation of DNA monolayers on gold surfaces. Analytical chemistry, 77(19), pp.6475-6480.

[6] Albers, J., Grunwald, T., Nebling, E., Piechotta, G. and Hintsche, R. (2003). Electrical biochip technology—a tool for microarrays and continuous monitoring. Analytical and bioanalytical chemistry, 377(3), pp.521-527.

[7] Clack, N., Salaita, K. and Groves, J. (2008). Electrostatic readout of DNA microarrays with charged microspheres. Nature biotechnology, 26(7), pp.825-830.

[8] Goodrich, T., Lee, H. and Corn, R. (2004). Enzymatically amplified surface plasmon resonance imaging method using RNase H and RNA microarrays for the ultrasensitive detection of nucleic acids. Analytical chemistry, 76(21), pp.6173-6178.

[9] Cao, Y., Jin, R. and Mirkin, C. (2002). Nanoparticles with Raman spectroscopic fingerprints for DNA and RNA detection. Science, 297(5586), pp.1536-1540.

[10] Bandiera, L., Cellere, G., Cagnin, S., De Toni, A., Zanoni, E., Lanfranchi, G. and Lorenzelli, L. (2007). A fully electronic sensor for the measurement of cDNA hybridization kinetics. Biosensors and Bioelectronics, 22(9), pp.2108-2114.

[11] Drummond, T., Hill, M. and Barton, J. (2003). Electrochemical DNA sensors. Nature biotechnology, 21(10), pp.1192-1199.

[12] Vo-Dinh, T., Alarie, J., Isola, N., Landis, D., Wintenberg, A. and Ericson, M. (1999). DNA biochip using a phototransistor integrated circuit. Analytical Chemistry, 71(2), pp.358-363.